Ultrasonics 53 (2013) 1104–1111

Contents lists available at SciVerse ScienceDirect

Ultrasonics

journal homepage: www.elsevier.com/locate/ultras

# Decision support system for ultrasound inspection of fiber metal laminates using statistical signal processing and neural networks

Eduardo F. Simas Filho [a,b,*], Yure N. Souza [a], Juliana L.S. Lopes [a], Cláudia T.T. Farias [a], Maria C.S. Albuquerque [a]

[a] Nondestructive Testing Research Group, Federal Institute of Bahia, 40301-015 Salvador, BA, Brazil
[b] Electrical Engineering Program, Federal, University of Bahia, 40210-630 Salvador, BA, Brazil

ARTICLE INFO

*Article history:*
Received 8 May 2012
Received in revised form 2 February 2013
Accepted 4 February 2013
Available online 21 February 2013

*Keywords:*
Ultrasound testing
Fiber–metal laminates composites
Neural networks
Principal Component Analysis
Independent Component Analysis

ABSTRACT

The growth of the aerospace industry has motivated the development of alternative materials. The fiber–metal laminate composites (FML) may replace the monolithic aluminum alloys in aircrafts structure as they present some advantages, such as higher stiffness, lower density and longer lifetime. However, a great variety of deformation modes can lead to failures in these composites and the degradation mechanisms are hard to detect in early stages through regular ultrasonic inspection. This paper aims at the automatic detection of defects (such as fiber fracture and delamination) in fiber–metal laminates composites through ultrasonic testing in the immersion pulse-echo configuration. For this, a neural network based decision support system was designed. The preprocessing stage (feature extraction) comprises Fourier transform and statistical signal processing techniques (Principal Component Analysis and Independent Component Analysis) aiming at extracting discriminant information and reduce redundancy in the set of features. Through the proposed system, classification efficiencies of ~99% were achieved and the misclassification of signatures corresponding to defects was almost eliminated.



## 1. Introduction

Fiber–metal laminate (FML) composites [1] consist of thin sheets of metal alternately bonded to thin layers of fiber-reinforced polymers [2]. FML have specific properties such as low density, resistance to impacts and corrosion [3] and thus are extensively used in the aerospace industry. The FML allow weight reduction and savings in fuel consumption and maintenance.

In order to monitor the integrity of these materials and identify the occurrence of failures, non-destructive methods [4], among which stands the ultrasonic testing [5,6], are applied. However, the multilayer structure of the FML produces ultrasonic signals of difficult analysis and interpretation, making the flaw detection process a difficult task. Considering this, the ultrasonic operators would benefit from an automatic decision support system designed to provide information on the FML integrity based on ultrasonic signals.

Some works have been developed in order to obtain automatic damages detection systems for composite laminate materials, such as [7] which proposes the use of a neural network classifier to detect damages based on the results of Acoustic Emissions non-destructive testing, or [8] which combines Digital Shearography non-destructive testing and unconstrained optimization methods to detect position and size of delaminations. The work [9] uses also a neural network for estimating the residual tensile strength after drilling in composite laminates. Neural network classifiers have also being use in [10–12] to detect welding defects based on ultrasonic testing. Unfortunately, there was not found a considerable effort on developing automatic flaws detection systems for fiber–metal laminate composites based on ultrasound testing.

Considering this, our work proposes a decision support system for ultrasound inspection of FML composites which comprises a neural network classifier [13] fed from frequency–domain information. An additional preprocessing step through statistical signal processing techniques (such as Principal Component Analysis – PCA [14] and Independent Component Analysis – ICA [15]) was also applied in order to properly select the classifier input features.

Neural network based classifiers are widely applied as they combine high discrimination efficiency, through nonlinear separation hyperplanes, and fast execution due to their parallelized structure [13]. Statistical signal processing (SSP) techniques were successfully employed for feature extraction in different applications such as high energy physics [16], passive sonar systems [17] and biomedical engineering [18]. In these cases, SSP proved to be an efficient preprocessing step for classification systems as it reduces the redundancy in the features set.

* Corresponding author at: Electrical Engineering Program, Federal, University of Bahia, 40210-630 Salvador, BA, Brazil. Tel.: +557132839772

*E-mail addresses:* eduardo.simas@ufba.br (E.F. Simas Filho), yuresouza@ifba.edu.br (Y.N. Souza), jlopes@ifba.edu.br (J.L.S. Lopes), cfarias@ifba.edu.br (C.T.T. Farias), cleaalbuquerque@ifba.edu.br (M.C.S. Albuquerque).

0041-624X/$ - see front matter © 2013 Elsevier B.V. All rights reserved.
http://dx.doi.org/10.1016/j.ultras.2013.02.005

This work is divided as follows. In Section 2 the main aspects of the fiber metal composites are briefly discussed. The proposed automatic flaws detection system is presented in Section 3. The applied signal processing chain is detailed in Section 4. The experimental results that validate the proposed approach are shown in Section 5. Finally, Section 6 brings the conclusions.

## 2. Fiber metal laminate composites

Composites are formed by the union of two or more materials with different characteristics in a way that their combination results in another material with specific mechanical properties.

The fiber metal laminate (FML) composites are formed by alternating layers of thin metal sheets and pre-impregnated material, which consists of fiber matrix and reinforcing agent.

The features of a composite depend on parameters such as fibers orientation in the matrix and the number of layers [1]. Table 1 shows the mechanical properties of different materials. It can be seen that the composites present high values of the elasticity module (**E**), while maintaining low density. Such mechanical properties are very important in several applications. Considering especially the aeronautic industry, weight reduction is one of the main advantages of composite materials. Other benefits over conventional structure include, high corrosion resistance, and increased resistance to damage from cyclic loading (fatigue).

### 2.1. Failure mechanisms

Fiber metal laminates exhibit failure mechanisms compatible with both metal and composite materials. The metallic sheets may develop fatigue crack growth (similar to monolithic metals). The fibers restrain the cracks but are subject to delamination at the metal–fiber interface (at the wake of the crack) due to cyclic shear stress [20]. Fig. 1 illustrates the effects of delamination and cracks in a composite material.

A fundamental aspect in composites is that, in general, a defect is produced through a gradual sequence of micro-cracks and delamination and thus, a composite material is subject to different kinds of flaws [21]. The occurrence of a certain type of defect depends on factors like: thickness, applied loads and the composite material characteristics. Traction loads usually cause ruptures in the fibers, while the compression loads produce defects like micro-buckling or shear.

Considering these complex modes of damage, it is important to properly evaluate the integrity of FML structures through some non-destructive testing technique. This is required in order to detect and monitor the evolution of flaws. The next section describes the automatic decision support system proposed in this work for ultrasound inspection of FML.

## 3. Proposed decision support system

The proposed decision support system comprises different signal processing steps. As illustrated in Fig. 2, initially, the ultrasonic signals are measured in a immersion pulse-echo configuration and digitalized by an oscilloscope.

**Table 1**
Comparison between the mechanical properties of different materials (here, $E$ is the elasticity module, $\sigma$ is the tension, E.F. means Elongation in Fracture and $\rho$ is the density) [19].

| Property | $E$ (GPa) | $\sigma$ (GPa) | E.F. (%) | $\rho$ (g/cm$^3$) |
|---|---|---|---|---|
| Glass fiber S | 87.0 | 3.5 | 4.0 | 2.5 |
| Kevlar | 180.0 | 3.45 | 1.9 | 1.5 |
| Carbon fiber AR | 250.0 | 2.8 | 1.2 | 1.8 |
| Carbon fiber AM | 370.0 | 1.7 | 0.5 | 1.9 |
| Carbon fiber AD | 230.0 | 4.5 | 2.0 | 1.8 |

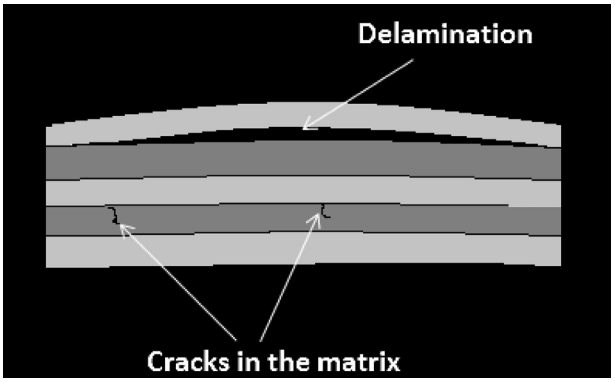


**Fig. 1.** Delamination and cracks in the matrix of fiber metal composite laminates.

The digital signal processing chain involves the Fourier transform, through the FFT (Fast Fourier Transform) algorithm [22]. In the following, the FFT coefficients are processed through statistical techniques (such as PCA [14] and ICA [15]) in order to remove statistical redundancy and reveal discriminating features. A supervised neural network based classifier [13] is used to produce an indication of the composite material integrity.

### 3.1. Ultrasonic testing in composites

Non-destructive testing techniques shall be used to evaluate the structural integrity of composites in equipments that require high level of reliability. Here, the ultrasonic testing have been used with this purpose due to the combination of simple execution and high efficiency in flaws identification [23]. However, the ultrasonic inspection efficiency in multi-layer composites may be limited by the internal structure of the material, specially when the specimen presents a large number of thin blades, which represent barriers and reflection surfaces for the acoustic wave propagation.

As the heterogeneous structure of the composites makes the conventional ultrasonic testing less reliable, the analysis of the ultrasonic signals through digital signal processing techniques enables better characterization of the acoustic signature, increasing echoes visibility and defects identification reliability [24,25].

### 3.2. Experimental setup

Considering that we are dealing with thin test objects (thickness of ~1.3 mm), the effect of the near field[1] prevents the use of a direct coupling. In this case, the immersion test is required in order to position the near field out of the testing zone.

In this work, as illustrated in Fig. 3, a water tank was used for immersion ultrasonic testing. The used inspection equipment comprises a Krautkramer USM-25® ultrasonic device and an Olympus Panametrics NDT V-326® transducer (diameter = 9.525 mm and nominal frequency = 5 MHz). In this initial version, the analog to digital (AD) conversion is performed using an oscilloscope (maximum sampling rate of 500 MHz) and the digital signal processing routines are executed in a personal computer. An upgraded version in which dedicated electronics (using a digital signal processor DSP) will replace both the oscilloscope and the computer is under development. In this setup, the AD conversion and the complete signal processing chain will be performed by the DSP based

[1] Area of high sonic interference, which hampers the detection of defects near the transducer.


**Fig. 2.** Block diagram of the proposed automatic evaluation system.

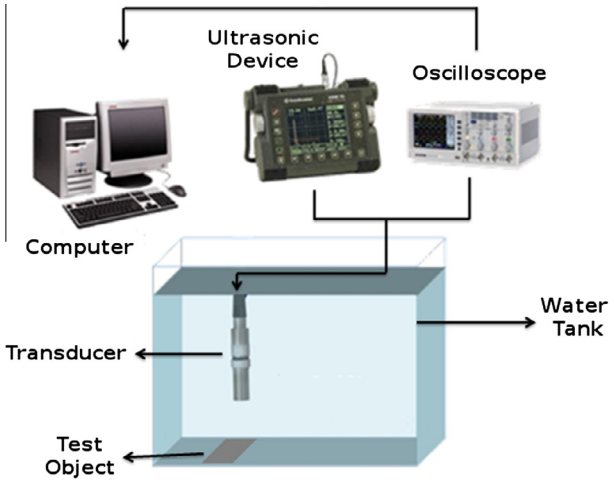


**Fig. 3.** Diagram of the experimental setup.

system.

The test objects used in this work are multi-layer composites comprising aluminum plates (100 mm × 100 mm × 0.5 mm) and pre-impregnated fiber uni-directionally reinforced (Hexply® 6376, 100 mm × 100 mm × 0.17 mm). The fibers orientation is parallel to the aluminum lamination direction. The used specimens present the following characteristics: no defect (ND), fiber fracture (F) and delamination (D). The defects were artificially introduced during the manufacturing process.

Fig. 4 illustrates the defective test objects. In the first specimen (Fig. 4-left) exists a fracture region in which a mesh of 8 × 10 points (with steps of 1.25 × 2 mm) was defined for signal acquisition. In a similar way, meshes of 10 × 10 points (using steps of 2 × 2 mm) were defined respectively for the delamination region (Fig. 4-right) and for the no defect region. Four different measurements were taken at each acquisition point in order to account for statistical variation.

## 4. The signal processing chain

Ultrasonic signals usually present low signal-to-noise ratio due to problems such as back-scattering (produced by reflection surfaces inside the test object) and noise (generated from acoustic and electronic sources) [26]. Considering this, a proper signal processing chain shall be applied to maximize the test efficiency. The

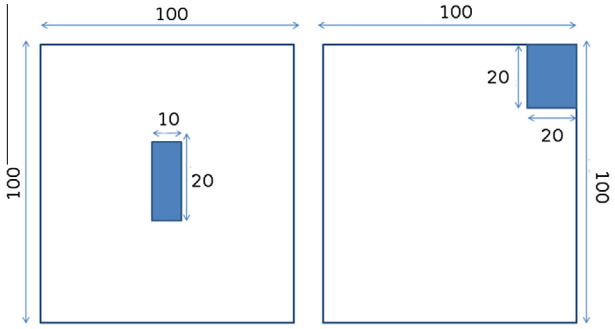


**Fig. 4.** Diagrams of the test objects (highlighting the defective regions), the dimensions are in mm.

different stages of the proposed signal processing chain are described further in this section.

### 4.1. Fourier analysis

Frequency domain analysis, through the Fourier transform, is widely used in ultrasound testing. When dealing with digital time-domain signals, the frequency components may be estimated through the Discrete Fourier Transform (DFT). The DFT $X\left(e^{j\frac{2\pi}{N}k}\right)$ of the time-domain signal $x[n]$ is defined as [22]:

$$X\left(e^{j\frac{2\pi}{N}k}\right) = \sum_{n=0}^{N-1} x[n]e^{-j\frac{2\pi}{N}kn} \tag{1}$$

for $0 \leqslant k \leqslant N-1$.

The acoustic signals characteristics are usually more evident in the frequency domain as it provides a more compact representation than the time-domain one. Furthermore, the effects of attenuation or scattering of the sound waves as they pass through a given material modify the frequency contents of the received pulses. Thus, frequency–domain information may be used to indicate the materials internal characteristics.

Considering this, ultrasonic testing involves the definition of reference standard signatures, which are determined from material with known characteristics, and the use of this baseline information to identify (or predict) the condition of the test samples.

### 4.2. Principal Component Analysis (PCA)

Principal Components Analysis (PCA) is a widely used technique for feature selection in statistical pattern recognition problems [14]. Considering a multivariate random vector $\mathbf{x} \in R^N$, the principal components may be estimated through singular value decomposition (SVD) [27] of the correlation matrix $\mathbf{R}$ of $\mathbf{x}$. This implies on solving the following equation system:

$$\mathbf{U}^T\mathbf{R}\mathbf{U} = \mathbf{\Lambda} \tag{2}$$

$$|\mathbf{U} - \lambda\mathbf{I}| = 0 \tag{3}$$

where $\mathbf{U}$ is an orthonormal matrix containing the eigenvectors of $\mathbf{R}$, $\mathbf{\Lambda}$ is a diagonal matrix, whose elements $\lambda_1, \lambda_2, \ldots, \lambda_N$ are the eigenvalues of $\mathbf{R}$, and $\mathbf{I}$ is the identity matrix. Once the eigenvectors are extracted, they can be ranked by their associated eigenvalues, forming the principal component projection base. Usually, prior to the PCA extraction, the random vector $\mathbf{x}$ is centralized by having its mean removed ($\mathbf{x} \leftarrow \mathbf{x} - \bar{\mathbf{x}}$), so that the correlation matrix becomes the covariance matrix. In such condition, the eigenvalues give the amount of energy (data variance) retained by the corresponding component.

Furthermore, PCA provides a projection matrix $\mathbf{U} \in R^{N\times N}$, where the components are uncorrelated and ranked by the amount of statistical variance they retain from $\mathbf{x}$. By discarding the least energetic components, one can achieve dimension reduction in an optimal way, in the mean squared error (MSE) sense.

### 4.3. Independent Component Analysis (ICA)

Considering that a set of $\mathbf{N}$ observed signals $\mathbf{x}(t) = [x_1(t), \ldots, x_N(t)]^T$ is generated by a linear combination of unknown sources $\mathbf{s}(t) = [s_1(t), \ldots, s_N(t)]^T$:

$$\mathbf{x}(t) = \mathbf{W}\mathbf{s}(t) \tag{4}$$

where $\mathbf{W}$ is the $N \times N$ mixing matrix [15].

The standard Independent Component Analysis (ICA) model deals with the problem of finding an estimate $\mathbf{y}$ of $\mathbf{s}$ considering that the components $y_i(t)$ are mutually statistically independent. A solution is obtained if one can find an approximation for the inverse of the mixing matrix $\mathbf{B} \approx \mathbf{W}^{-1}$ and so:

$$\mathbf{s}(t) \approx \mathbf{y}(t) = \mathbf{B}\mathbf{x}(t) \tag{5}$$

There are many mathematical methods for estimating the elements $(b_{ij})$ of $\mathbf{B}$ considering that the mutual independence assumption between the $y_i$ holds. The nonlinear decorrelation and the maximally nongaussianity are among the most applied ones [28].

While PCA explores second order statistics and removes signal correlation, ICA uses also higher-order information to produce statistical independence. Indeed, some ICA algorithms use PCA as a preprocessing step. Considering that after PCA all second order dependence is removed, the ICA problem is partially solved and it is only needed to deal with the higher order statistics information. ICA have been successfully applied for feature extraction in [16,29].

In this work the FastICA algorithm [28] was applied for independent components estimation. The Fast Fixed-Point Algorithms so called FastICA were derived through approximate Newton-type iterations applied to optimize a criterion based on parameters from information theory such as the negentropy [30]. Among the advantages of the method we can mention fast and more reliable convergence (if compared to gradient based algorithms), computational simplicity and little memory requirements.

### 4.4. Neural classification

Artificial Neural Networks (ANN) are computational models inspired in the human brain behavior. Basically, an ANN is composed of several (usually nonlinear) processing units called neurons, which may be interconnected in a highly complex and parallel way. Some important features of the ANNs are listed below:

- Learning: through the training procedure the network is capable of learning from the input dataset.
- Generalization: the acquired knowledge shall be applied on data not present in the training set.
- Adaptivity: the ANN can adapt their synaptic weights to changes in the environment.
- Fault tolerance: a neural network is inherently robust to missing data and additive noise due to the distributed nature of the acquired knowledge.

An artificial neuron model is illustrated in Fig. 5. The input signals $(x_1, x_2, \ldots, x_n)$ may represent external sensor units or the outputs of other neurons. The neuron synaptic weights $(\omega_0, \omega_1, \ldots, \omega_n)$ are adjusted during the training procedure and thus, retain the acquired knowledge. The nonlinear activation function $\phi(\cdot)$ allows access to high order statistical information [31]. The neuron output $y$ is defined as:

$$y = \phi\left(\sum_{i=1}^{n} \omega_i x_i + \omega_0\right) \tag{6}$$

The mapping (approximation) capabilities of a single neuron are limited and thus, for solving complex problems a neural network with multiple neurons is required. A multi-layer perceptron (MLP) neural network comprises a feed-forward cascaded structure of neuron layers and is proved to be an universal approximator. For MLP neural networks, error back-propagation algorithms are usually applied in the training phase [13].

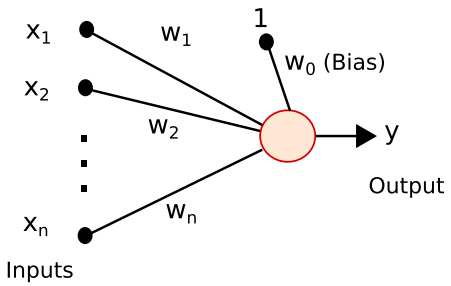


**Fig. 5.** Artificial neuron model.

In this work, multi-layer perceptron (MLP) neural networks comprising input, hidden and output layers were used as classifiers. The input layer connects the network to the features used in the discrimination problem and the output layer produces the decision. The hidden layer is responsible to produce the hyperplanes that separate the classes of interest. The hyperbolic tangent activation function was used in all neurons.

## 5. Results

To design and test the proposed system, the available experimental data was equally split into training, validation and testing sets. In order to properly explore the available statistics, the neural network training procedure was initialized 10 different times randomly choosing the signals that compose each dataset (training validation and testing).

To evaluate the obtained discrimination performance the normalized efficiencies product (EP) and the confusion matrix were used. Considering a three-class problem the EP shall be defined as:

$$\mathrm{EP} = (Ef_1 \times Ef_2 \times Ef_3)^{1/3} \tag{7}$$

where $Ef_i$ is the discrimination efficiency for the $i$th class of interest. This index is interesting due to its sensitivity to changes in the efficiencies of all classes. When EP = 1 maximum efficiency is achieved (100% of accuracy).

The elements $(c_{ij})$ of the confusion matrix $(\mathbf{C})$ represent the amount (usually in %) of signals from class $i$ identified by the classifier as belonging to class $j$. Considering this, the diagonal brings the efficiencies ($c_{ii} = Ef_i$) and the off-diagonal elements represents misclassification. When maximum efficiency is achieved the confusion matrix tends to a diagonal matrix.

As described previously in Section 4, the initial digital signal processing step consists on converting the acquired signals to the frequency domain. Fig. 6 presents the average Fourier spectra[2] for the tree classes of interest: no defect, delamination and fracture. It is possible to observe that the average events present similar characteristics with slight differences in the bandwidth (specially for the delamination case that presents a quite larger frequency band) and in the frequency profile shape (the no defect mean signal presents a local minimum point around 6 MHz). It can also be depicted that the frequency–domain information is close to zero in a large band (specially for frequencies > 10 MHz).

In the next signal processing step, the frequency–domain information (corresponding to 256 coefficients) is projected into the principal components. As it can be observed in the PCA load curve (see Fig. 7), high compaction rates were achieve, in a way that, the 1st, 5th and 15th most energetic principal components retain respectively 86.2%, 97.7% and 99.5% of the total signal energy and represent compaction rates of 256×, ∼51× and ∼17×.

[2] The average spectra are obtained by computing, for each class, the mean of all DFT signatures in the training set.

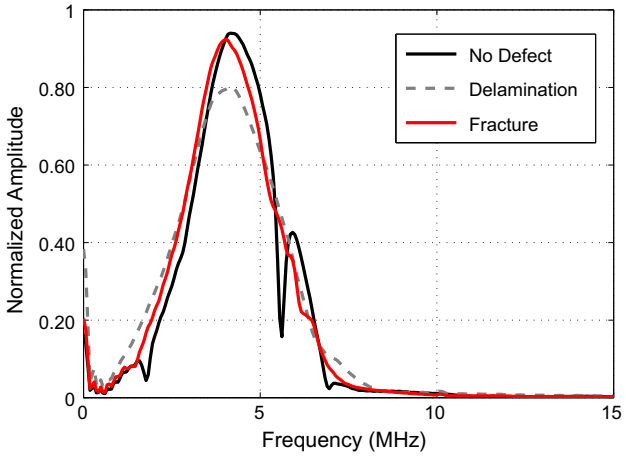


**Fig. 6.** Average Fourier spectra for the different classes of interest.

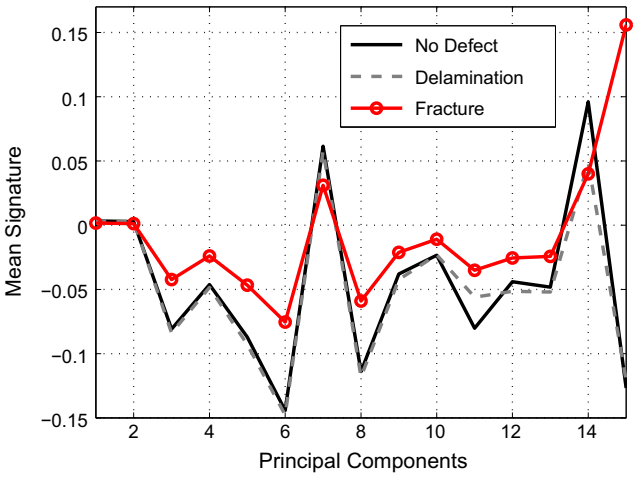


**Fig. 8.** Average events considering the first 15 principal components.

Fig. 8 shows the average events for each class when the DFT coefficients are projected into the 15 more energetic principal components. It can be observed that the similarity between delamination and no defect signals is preserved in the principal components, but, using PCA, the mean profile of fracture signals is more easily distinguished from the others. This indicates that the discriminating information present in the 256 frequency coefficients is somehow highlighted in these 15 principal components. It is also important to notice that due to singularity in the covariance matrix (of the DFT coefficients), the PCA algorithm was able to estimate only 80 principal components. A possible reason for this is that a large number of DFT coefficients tends to zero.

Using the information provided by PCA, an Independent Component Analysis (ICA) algorithm (Fast ICA [28]) was applied in order to estimate the ICA transformation.

Considering the different preprocessing steps (DFT, DFT + PCA and DFT + ICA), linear discriminators [31] were trained to each case in order to evaluate whether the classification problem requires a more complex (nonlinear) classifier (such as a neural network) or it can be properly solved linearly. In this case, 80 components were used for both PCA and ICA (which corresponds to a compaction factor of 3.2 and retains almost 100% of the signal energy).

The linear classifier was implemented using a single layer neural network structure with three linear neurons. The $i$th neuron was trained with target output equal to 1 for signatures belonging to class $i$ and $-1$ otherwise. In the operation phase, for a given input signal, the neuron which produces highest output value indicates the assigned class.

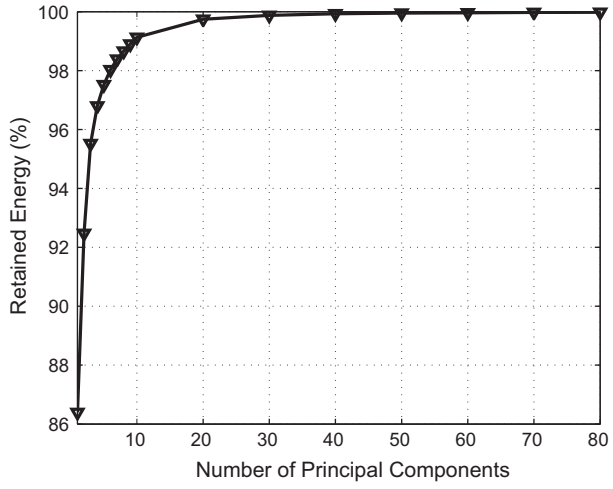


**Fig. 7.** Obtained PCA load curve.

Table 2 illustrates the discrimination efficiencies (considering both the EP and the confusion matrix). obtained by feeding a linear discriminator directly from the frequency domain coefficients (DFT). A particular characteristic of our application is that the misclassification of signals corresponding to defects as no defect signatures is more serious than the opposite case, because this mistake may seriously compromise the system reliability. For the linear classifier it was obtained EP = 0.8011 ± 0.3590 and high confusion among the different classes. In this case ∼29% of the signals corresponding to defects (delamination and fracture) were incorrectly classified as having no defect.

When the linear discriminator is fed from the principal components (DFT + PCA) a significant improvement in the discrimination efficiencies was achieved. In this case, EP = 0.9896 ± 0.0113 and the confusions (classification errors) were <2%. The misclassification of defects signatures as having no defect was reduced to ∼1.2%.

If the Independent Component Analysis (DFT + ICA) was applied, the discrimination efficiency was slightly increased (EP = 0.9945 ± 0.0065). In this case, the misclassification of defects is almost eliminated (∼0.08%) and the fracture signatures were identified with no error. Fig. 9 illustrates the independent components (IC) discrimination capability. Considering the projection in the first IC, the fracture signatures are linearly separable from the other classes, allowing full identification of this pattern using a linear classifier. The IC projections also provide low confusion among no defect and delamination signatures, as it can be observed from the 73rd IC projections for these classes.

**Table 2**
Confusion matrices (in %) for delamination (D), fracture (F) and no-defect (ND) regions considering a linear classifier for different signal processing chains.

| | D | F | ND |
|---|---|---|---|
| *DFT (256 comp./EP = 0.8011 ± 0.3590)* | | | |
| D | 70.2079 | 11.8879 | 17.9042 |
| F | 9.2696 | 79.7819 | 10.9484 |
| ND | 5.0833 | 2.8716 | 92.0451 |
| *DFT + PCA (80 comp./EP = 0.9896 ± 0.0113)* | | | |
| D | 97.7307 | 1.5637 | 0.7056 |
| F | 0.0926 | 99.4444 | 0.4630 |
| ND | 0.2459 | 0 | 99.7541 |
| *DFT + ICA (80 comp./EP = 0.9945 ± 0.0065)* | | | |
| D | 99.9219 | 0 | 0.0781 |
| F | 0 | 100 | 0 |
| ND | 3.4447 | 0 | 96.5553 |

In a neural discriminator, the number of neurons in the hidden layer (HN) is a parameter that needs to be specified during the design process. HN usually increases with the complexity of the problem. In this work, an iterative experimental procedure was applied in order to determine the "optimum" value for HN. For this, a classifier with a single hidden neuron was trained (HN = 1) and the respective value of EP computed. In the following, the number of hidden neurons was increased to HN = 2 and the training procedure restarted. These iterations continue until there is no significant improvement in the discrimination efficiency by adding new neurons.

Fig. 10 illustrates the variation of EP as a function of HN for both DFT and DFT + PCA preprocessing (the curve obtained for the DFT + ICA case was very similar to the DFT + PCA one and was omitted for simplicity). One can see that for HN = 4 the efficiency (measured by EP) achieved approximately its maximum value. Considering this, neural classifiers with four hidden neurons were used in further analysis. Other important aspect is that through PCA and ICA preprocessing it was possible o achieve high discrimination efficiencies even for a small number of hidden neurons, indicating that the proposed preprocessing somehow reveals the relevant information, facilitating flaws identification.

Table 3 shows the results obtained by feeding neural (multilayer perceptron) classifiers after different preprocessing steps. It

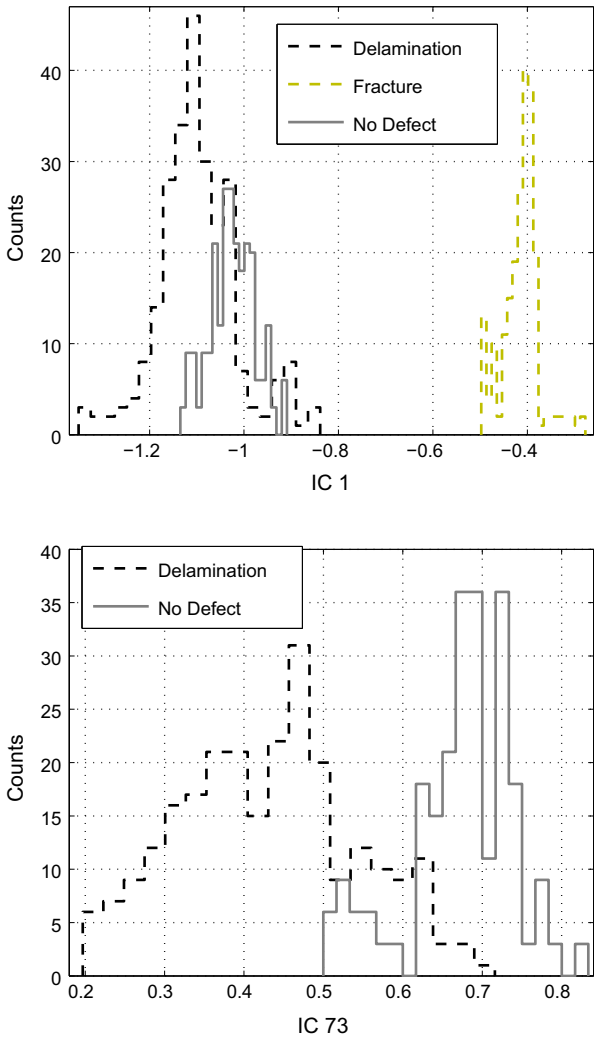


**Fig. 9.** Distributions of the first (top) and 73rd (bottom) independent components for the classes of interest.

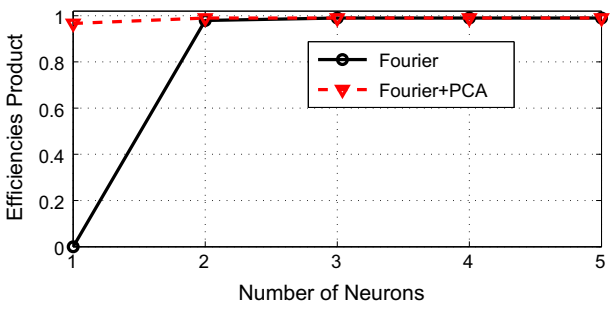


**Fig. 10.** Normalized efficiencies product as a function of the number of hidden neurons in the neural classifier.

can be seen that the neural classifier is able to produce high discrimination efficiency for all cases. It can also be observed that for PCA and ICA preprocessing the fracture signals are identified without confusion. The highest EP was obtained by the discriminator fed from the independent components (EP $\sim$ 0.998). In this case, the misclassification of defects signatures was as low as $\sim$0.16%. This indicates that the statistical independence obtained after ICA favors signal identification for all classes of interest.

It is also important to note the efficiency of PCA for signal compaction. By training a neural discriminator only from the five most energetic principal components it was also possible to obtain high discrimination efficiency (see Table 4), achieving EP $\sim$ 0.993 and confusion probabilities lower than 1.3%. In this case, a classifier with only two hidden neurons was able to produce the highest discrimination efficiency. This result is very important if the proposed system is embedded in portable inspection equipment, as a reliable indication is obtained by using low computational requirements.

An estimate of the computational requirements of the proposed discriminators may be obtained by analyzing the number of multiplications and accumulations (MAC) required after the DFT computation (which is common in all cases), to provide the final decision.

In a general configuration, the input DFT feature vector $\mathbf{x}$ is multiplied by a matrix $\mathbf{U}$. which was defined for PCA or $\mathbf{B}$ for the ICA case (in this computational requirements analysis only the $\mathbf{U}$ matrix is used, without loss of generality). A neural network with two layers produces the final output $y$ through:

$$y = F(\mathbf{W_2}F(\mathbf{W_1}\mathbf{U}\mathbf{x})) \tag{8}$$

where $\mathbf{W_1}$ and $\mathbf{W_2}$ are respectively the neural network input and hidden layers weights and $F(\cdot)$ is the activation function. As in the operational phase, $\mathbf{U}$, $\mathbf{W}_1$ and $\mathbf{W_2}$ are known in advance, it is possible to previously compute the product $\mathbf{U_1} = \mathbf{U}\mathbf{W_1}$ and so, Eq. (8) may be modified to:

**Table 3**
Confusion matrices (in %) for delamination (D), fracture (F) and no-defect (ND) regions considering a MLP neural classifier (HN = 4) for different signal processing chains.

| | D | F | ND |
|---|---|---|---|
| *FFT (256 comp./EP = 0.9970 ± 0.0054)* | | | |
| D | 99.6094 | 0.0781 | 0.3125 |
| F | 0 | 100 | 0 |
| ND | 0.4918 | 0 | 99.5082 |
| *FFT + PCA (80 comp./EP = 0.9966 ± 0.0035)* | | | |
| D | 98.9831 | 0 | 1.0196 |
| F | 0 | 100 | 0 |
| ND | 0 | 0 | 100 |
| *FFT + ICA (80 comp./EP = 0.9978 ± 0.0053)* | | | |
| D | 99.8438 | 0 | 0.1563 |
| F | 0 | 100 | 0 |
| ND | 0.4918 | 0 | 99.5082 |

**Table 4**
Confusion matrix (in %) for delamination (D), fracture (F) and no-defect (ND) regions considering a MLP classifier fed from the five more energetic principal components.

| | D | F | ND |
|---|---|---|---|
| *FFT + PCA (5 comp./EP = 0.9932 ± 0.0155)* | | | |
| D | 99.2169 | 0 | 0.7831 |
| F | 1.2150 | 98.7850 | 0 |
| ND | 0 | 0 | 100 |

**Table 5**
Comparison between different discriminators considering EP, misclassification of defects (Miss Def. in %) and the number of MACs.

| Preproc. | EP | Miss Def. | MACs |
|---|---|---|---|
| *Linear classifier* | | | |
| DFT | 0.8011 | 28.85 | 768 |
| $PCA_{(80comp.)}$ | 0.9896 | 1.17 | 768 |
| ICA | 0.9945 | 0.08 | 768 |
| *Neural classifier* | | | |
| DFT | 0.9970 | 0.31 | 1225 |
| $PCA_{(80comp.)}$ | 0.9966 | 1.02 | 1225 |
| $PCA_{(5comp.)}$ | 0.9932 | 0.78 | 653 |
| ICA | 0.9978 | 0.16 | 1225 |

$$y = F(\mathbf{W_2}F(\mathbf{U_1}\mathbf{x}))) \tag{9}$$

Considering that the feature vector $\mathbf{x}$ has 256 coefficients, the number of MACs is for the linear classifier is computed through: $N_{MAC} = 256 \times 3$. For the MLP classifiers, the number of MACs is a function of the number of hidden neurons NH. The nonlinear neurons also require the computation of the hyperbolic tangent (tan$h$) activation function, which shall be performed accurately using Taylor series expansion [32]. For a seven terms expansion approximately 27 MACS are required for each tan$h$ computation. In this case: $N_{MAC} = 256 \times NH + NH \times 3 + (NH + 3) \times 27$.

Table 5 provides a comparison between the proposed discriminators considering the discrimination efficiency, the misclassification of defects and the computational requirements estimation. Generally, the used MLP classifiers presented NH = 4, except for the MLP classifier fed from the five principal components ($PCA_{(5comp.)}$), which used NH = 2 It can be seen that linear discriminators present reduced computational requirements, together with the $PCA_{(5comp.)}$ based nonlinear discriminator. It can also be observed that for both linear and nonlinear classifiers, best results were obtained after ICA preprocessing. Furthermore, the ICA based discriminators presented minimum misclassification of defects signatures, which is very important to the reliability of the proposed decision support system.

## 6. Conclusions

The fiber metal laminates (FML) are very important materials in many applications (specially in the aeronautic industry) due to features such as high stiffness, low density and long lifetime. However, its various modes of deformation and its physical structure in multiple layers make the detection of flaws in early stages a difficult task. In this work was proposed an automatic decision support system to help the inspector in the identification of different kinds of defects that may appear in FMLs. For this, a signal processing chain which comprises two distinct stages (feature extraction and hypothesis testing) was designed. For feature extraction, the acquired signals were transformed to the frequency domain and processed by statistical techniques (such as PCA and ICA) in order to remove redundancy and reduce the background noise. The hypothesis testing (classification) stage was performed by both linear and neural classifiers. The applied feature extraction techniques were able to reveal the underlying structure of the data producing high discrimination efficiencies. This can be observed particularly when a linear discriminator was used. In this configuration, the efficiency was considerably improved by using PCA and ICA transformations. In the case of ICA preprocessing, the classification results were quite similar to the ones achieved when using the nonlinear (neural) discriminators, but with considerably lower computational requirements. Considering the neural classifiers, the ICA preprocessing also contributes to produce higher discrimination efficiencies, achieving EP = ~0.998 and reducing the misclassification of defect signals to ~0.16%. In this context, PCA proved to be also very efficient for signal compaction as a neural discriminator fed from only the five most energetic components was able to present high discrimination accuracy (EP = ~0.993).

## Acknowledgments

The authors would like to express their gratitude to FAPESB and IFBA for the financial support and to GPEND members for the fruitful discussions concerning this work.

## References

[1] A. Vlot, J.W. Gunnink (Eds.), Fibre Metal Laminates – An Introduction, Springer, 2001.
[2] E.K. Baumert, W.S. Johnson, R.J. Cano, B.J. Jensen, E.S. Weiser, Mechanical evaluation of new fiber metal laminates made by the VARTM process, in: Proceedings of the International Conference on Composite Materials, Edinburgh, UK, 2009, pp. 1–12.
[3] M. Hagenbeek, C. Van Hengel, O. Bosker, C.A.J.R. Vermeeren, Static properties of fibre metal laminate, Applied Composite Materials 10 (2003) 207–222.
[4] C.H. Hellier, Handbook of Nondestructive Evaluation, second ed., McGraw-Hill, 2012.
[5] C.H. Chen (Ed.), Ultrasonic and Advanced Methods for Nondestructive Testing and Material Characterization, World Scientific, 2007.
[6] L.W. Schmerr, S.J. Song, Ultrasonic Nondestructive Measurement Systems – Models and Measurements, Springer, 2007.
[7] T.P. Philippidis et al., Damage characterization of carbon/carbon laminates using neural network techniques on AE signals, NDT & E International 31 (5) (1998) 329–340.
[8] G. De Angelis et al., A new technique to detect defect size and depth in composite structures using digital shearography and unconstrained optimization, NDT & E International 45 (1) (2012) 91–96.
[9] R. Mishr et al., Neural network approach for estimating the residual tensile strength after drilling in uni-directional glass fiber reinforced plastic laminates, Materials & Design 31 (6) (2010) 2790–2795.
[10] A. Masnata, M. Sunseri, Neural network classification of flaws detected by ultrasonic means, NDT & E International 29 (2) (1996) 87–93.
[11] I. Souza, M.C. Albuquerque, E. Simas Filho, C. Farias, Signal processing techniques for ultrasound automatic identification of flaws in steel welded joints – a comparative analysis, in: World Conference on Nondestructive Testing, Durban, South Africa, 2012.
[12] S. Legendre et al., Neural classification of Lamb wave ultrasonic weld testing signals using wavelet coefficients, IEEE Transactions on Instrumentation and Measurement 50 (3) (2001) 672–678.
[13] S. Haykin, Neural Networks and Learning Machines, third ed., Prentice Hall, 2008.
[14] I.T. Jolliffe, Principal Component Analysis, Springer, 2002.
[15] A. Hyvarinen, J. Karhunen, E. Oja, Independent Component Analysis, Wiley, 2001.
[16] E.F. Simas Filho, J.M. Seixas, L.P. Caloba, Modified post-nonlinear ICA model for online neural discrimination, Neurocomputing 73 (16–18) (2010) 2820–2828.
[17] N.N. Moura, E.F. Simas Filho, J.M. Seixas, Independent component analysis for passive sonar signal processing, in: Sergio Rui Silva (Ed.), Advances in Sonar Signal Processing, In-Tech, Viena, Austria, 2009, pp. 91–110.
[18] J. Escudero, R. Hornero, et al., Artifact removal in magneto-encephalogram background activity with independent component analysis, IEEE Transactions on Biomedical Engineering 54 (11) (2007) 1965–1973.
[19] C. Zweben, H.T. Hahn, T.W. Chou, Mechanical Behavior and Properties of Composite Materials, second ed., Technomic Publishing Company, 1989.
[20] S. Abdullah, A. Fahruddin, J. Syarif, M.Z. Omar, R. Zulkifli, Fatigue crack growth modelling of fibre metal laminate (FML) composite, European Journal of Scientific Research 35 (1) (2009) 43–53.
[21] Dennis A. Burianek, Dong-Jin Shim, S. Mark Spearing, Durability of hybrid fiber metal composite laminates, in: Proceedings of the International Conference on Fracture, Turin, Italy, March 20–25, 2005, pp. 1–5.
[22] P.S.R. Diniz, E.A.B. da Silva, S.L. Netto, Digital Signal Processing: System Analysis and Design, Cambridge University Press, Cambridge, UK, 2010.

[23] W.J. Lee, W.V. Chang, W. Yang, B. Kim, Defects detection using a smart ultrasound pulse-echo technique, Polymer Composites (2009).
[24] R. Kazys, L. Svilanis, Ultrasonic detection and characterization of delaminations in thin composite plates using signal processing techniques, Ultrasonics 35 (1997) 367–383.
[25] R. Drai, A. Benammar, Ultrasonic signal processing in the detection of defect in composite, in: European Conference of Non Destructive Testing, Berlin, Alemanha, 2006.
[26] J. Chen et al., Noise analysis of digital ultrasonic nondestructive evaluation system, International Journal of Pressure Vessels and Piping (76) (1999) 619–630.
[27] D.C. Lay, Linear Algebra and Its Applications, fourth ed., Addison Wesley, 2011.
[28] A. Hyvarinen, E. Oja, Independent component analysis: algorithms and applications, Neural Networks 13 (4–5) (2000) 411–430.
[29] K.C. Kwak, W. Pedrycz, Face recognition using an enhanced independent component analysis approach, IEEE Transactions on Neural Networks 18 (2) (2007) 530–541.
[30] T.M. Cover, J.A. Thomas, Elements of Information Theory, Wiley, New York, 1991.
[31] R.O. Duda, P.E. Hart, D.G. Stork, Pattern Classification, second ed., Wiley, 2000.
[32] M. Avci, T. Yildirim, Generation of tangent hyperbolic sigmoid function for microcontroller based digital implementations of neural networks, in: International Turkish Symposium on Artificial Intelligence and Neural Networks, 2003, pp. 1–5.